Magyarhoni Földtani Társulat
Földtani Közlöny
Hungarian Geological Society

154/3, 267–276., Budapest, 2024

DOI: 10.23928/foldt.kozl.2024.154.3.267

K-feldspar – H_2 interaction in the context of underground hydrogen storage

Gelencsér, Orsolya[1,2,3,*], Szabó-Krausz, Zsuzsanna[1], Németh, Tibor[4,5], Árvai, Csaba[6], Mika, László Tamás[6], Kővágó, Ákos[1,7], Breitner, Dániel[8], Tóth, Péter[3], Falus, György[1,9]

[1]ELTE Eötvös Loránd University, Institute of Geography and Earth Sciences, Department of Petrology and Geochemistry, Lithosphere Fluid Research Lab; [2]Doctoral School of Environmental Sciences, Faculty of Science, ELTE Eötvös Loránd University; [3]O&GD Central Ltd. Budapest; [4]Department of Meteorology, University of Pécs; [5]ELTE Eötvös Loránd University, Institute of Geography and Earth Sciences, Department of Mineralogy; [6]Department of Chemical and Environmental Process Engineering, Faculty of Chemical Technology and Biotechnology, Budapest University of Technology and Economics; [7]HUN-REN Institute of Earth Physics and Space Science, Sopron; [8]Green Ventures Ltd. Budapest; [9]Supervisory Authority for Regulatory Affairs, Budapest, Hungary

*Corresponding author: gecso@staff.elte.hu

Káliföldpát – hidrogén kölcsönhatás a felszín alatti hidrogéntárolás összefüggésében

Összefoglalás

A geológiai rezervoárok, beleértve a homokkőtesteket, meghatározó szerepet kaphatnak a felszín alatti hidrogéntárolásban. Ennek megvalósításához szükség van a kőzet pórusterében a hidrogéninjektálás hatására végbemenő kémiai reakciók megismerésére is. A földpátok gyakori kőzetalkotók, és a pH változására könnyen mállanak. Tanulmányunkban áztatásos kísérletekkel és geokémiai modellezéssel vizsgáltuk a nagy nyomású hidrogén K-földpátra gyakorolt geokémiai hatását felszín alatti tároló körülmények között (100 bar, 105 °C). Az áztatásos kísérletekben az oldatot mintázva követtük a káliföldpát oldódását. A kísérleti adatok alapján a káliföldpát – víz – hidrogén rendszerben kismértékű eltérést tapasztaltunk a referenciakísérlethez képest, amelyekben inert nitrogént használtunk. A hidrogén hatására kezdetben intenzívebb K- és Na-oldódást tapasztaltunk, míg az Al és Si átlagosan kevesebb a referenciakísérletekhez képest. A kinetikus PHREEQC-modellek a káliföldpát hasonló mértékű oldódását mutatják mindkét rendszerben. Összességében elmondható, hogy a káliföldpát nem különösebben reaktív hidrogén jelenlétében. Mindazonáltal a rezervoár körülményeken végzett kísérletek és a végbemenő reakciók modellezése egyértelmű előrelépés a változatos ásványokból álló üledékes rezervoár kőzetek hidrogéntárolási képességének megismerésében.

Tárgyszavak: káliföldpát, felszín alatti hidrogéntárolás, geokémiai modellezés, áztatásos kísérlet

Abstract

Geologic reservoirs, including sandstones, can serve as sites for underground hydrogen storage (UHS). However, for a successful commercial application, a more detailed knowledge of the rock–pore-water–hydrogen gas (H_2) systems is necessary. In this combined experimental-modeling study, the geochemical impact of H_2 on K-feldspar was investigated. Static batch reactor experiments were conducted under pressure and temperature conditions of potential UHS to track the effect of H_2 on K-feldspar. The experimental data show a negligible reactivity of K-feldspar. The kinetic PHREEQC model predicts the dissolution of K-feldspar to a similar extent as suggested by the experimental observations. Findings of this study show that the K-feldspar–H_2 interaction is marginal. The results mark clear progress in understanding the chemical changes in polymineralic reservoir rock matrix during hydrogen injection processes.

Keywords: K-feldspar, underground hydrogen storage, geochemical modeling, batch experiment

Introduction

There is growing interest within the energy industry in utilizing subsurface porous media stemming from various factors, including the need for efficient storage of energy resources (e.g., natural gas, compressed air, and hydrogen). Additionally, advancements in technology, such as the development of geothermal energy systems, CO_2 capture and storage (CCS), enhanced oil recovery (EOR) techniques have further fueled interest in understanding and utilizing subsurface porous media for various energy-related purposes. Hydrogen storage as well as CCS and nuclear waste disposal are imminent technologies that are still facing the challenge of unpredicted rock-water-gas interactions in

porous media. Geologic storage of resources, including H_2, can be successful only if the geochemical and microbial interactions between injected gas, host-rock and formation brines are adequately understood (YEKTA et al. 2018, HEINEMANN et al. 2021, AL-YASERI et al. 2023). In geologic formations, the feldspar group minerals have drawn the attention of applied geochemical studies as feldspars are common minerals that are found both in porous sandstone formations and clay caprocks (YUAN et al. 2019, ZIVAR et al. 2021).

Feldspars are substantial constituents of the Earth's crust (CHARDON et al. 2006) and are widely distributed on other planetary bodies of the inner Solar System (BEHRENS 2021). Their high abundance on the Earth is due to their wide range of stability and various ways of their formation (e.g., magmatic, volcanic, hydrothermal) (CHARDON et al. 2006). Chemical weathering of feldspars influences the groundwater flow and chemistry as their dissolution and precipitation can affect the porosity and permeability of aquifers (WELCH & ULLMAN 1996). Surface reactions of feldspars are of particular importance in soil development (LIU et al. 2017, MANNING et al. 2017) and can have effects on global climate change by buffering atmospheric CO_2 (BERNER 1995). They also have economic importance since feldspar is used in the construction industry (glass and ceramic products, cements) for its alumina and alkali content (FUERTES et al. 2022).

The feldspar group of silicate minerals is characterized by three-dimensional framework structure, which is able to accommodate K, Na, Ca in AlO_4 and SiO_4 tetrahedral network (RIBBE 1994). Feldspars not only rank as the most abundant minerals in the Earth's crust, but also exhibit a wide range of structural variations, which can be observed in rocks with diverse cooling histories (BENISEK et al. 2004). The major elements in feldspars can be expressed as mineral series with three endmembers – $KAlSi_3O_8$ (K-feldspar) – $NaAlSi_3O_8$ (albite) – $CaAl_2Si_2O_8$ (anorthite). Solid solutions between K and Na endmembers exist, similarly between Na and Ca, however it is very limited between K and Ca (PUTNIS 1992, FUERTES et al. 2022).

In this paper, we investigate feldspar alteration in the context of subsurface hydrogen storage using the knowledge of previously collected extensive feldspar-related geochemical studies and applying the approach used for an earlier investigation of calcite reactivity under geologic storage conditions (GELENCSÉR et al. 2023). The study of rock-forming mineral reactivity in the context of hydrogen storage is a constantly evolving field of applied geochemistry. Experiments are necessary to reproduce mineral–H_2 interactions in aqueous media, although they carry the disadvantage of representing limited time and space. Geochemical models are widely used in geochemistry to simulate chemical reactions that occur in natural reservoirs, such as gas storage in geological formations. The simultaneous application of experimental and modeling work is one of the most efficient ways to predict the possible effects of mineral–H_2 interactions under reservoir conditions.

Materials and methods

Starting material

A homogenous feldspar, provided by the Eötvös Museum of Natural History, Eötvös Loránd University (ID: BE40767) was used as the substrate of the experimental study. The purity of the feldspar sample was verified by optical and scanning electron microscopy (lack of perthite, rarity of fluid and solid inclusions) and X-ray powder diffraction. The chemical composition was determined by chemical analysis. For the experiments, the feldspar was crushed and powdered, and grains were selected with a particle size between 100 and 200 μm by the use of wet sieving. The powder with corresponding grain size was cleaned ultrasonically in distilled water, then it was dried and handpicked to remove any impurities before the experiments.

Thin sections of the sieved feldspar grains were prepared for physical (optical) and chemical analyses. They were also coated with carbon for scanning electron microscopic investigation. A feldspar sample was also prepared for X-ray powder diffraction analysis.

The liquid samples of experiments were filtered through a 0.2 μm syringe filter and were mixed with ca. 5 mL of 1 wt.% HNO_3 solution. The sealed samples were stored in scintillation vials until subsequent analysis.

Optical microscopy was applied on the prepared thin sections to observe differences between treated and untreated K-feldspar grains. For this purpose, stereo (Nikon® SMZ 800) and polarized microscopes (Nikon® Eclipse E600POL) were used in the Lithosphere Fluid Research Lab (LRG), Eötvös Loránd University (ELTE), Budapest.

X-ray powder diffraction (XRPD) measurements were performed on a powdered sample at the Department of Mineralogy (Eötvös University), using a Siemens D5000 diffractometer, for structural determination of the mineral. The instrument was operated with the following conditions: 45 kV, 35 mA, Cu Kα-radiation, graphite monochromator, 0.05° 2 step size, 2 sec detection time.

To obtain the major elemental composition of the K-feldspar, a Hitachi TM4000Plus scanning electron microscope equipped with Oxford AZtec One 30mm^2 SDD energy dispersive spectrometer (SEM-EDX) was used at the Center for Research and Industrial Relations, ELTE, Budapest. The accelerating voltage was set at 15 kV and the beam current was 200 pA.

Experimental procedure

Two types of experiments were conducted:

Type-1: The K-feldspar–H_2O–H_2 batch experiments were performed in 160 mL Hastelloy Steel High-pressure Parr® reactors. The experimental procedure followed the description of GELENCSÉR et al. (2023) as 2 g cleaned mineral, and 70 mL of distilled water were placed into the reactor followed by its pressurization up to 80 bar for both H_2 and N_2 containing experiments. The reaction mixture was then

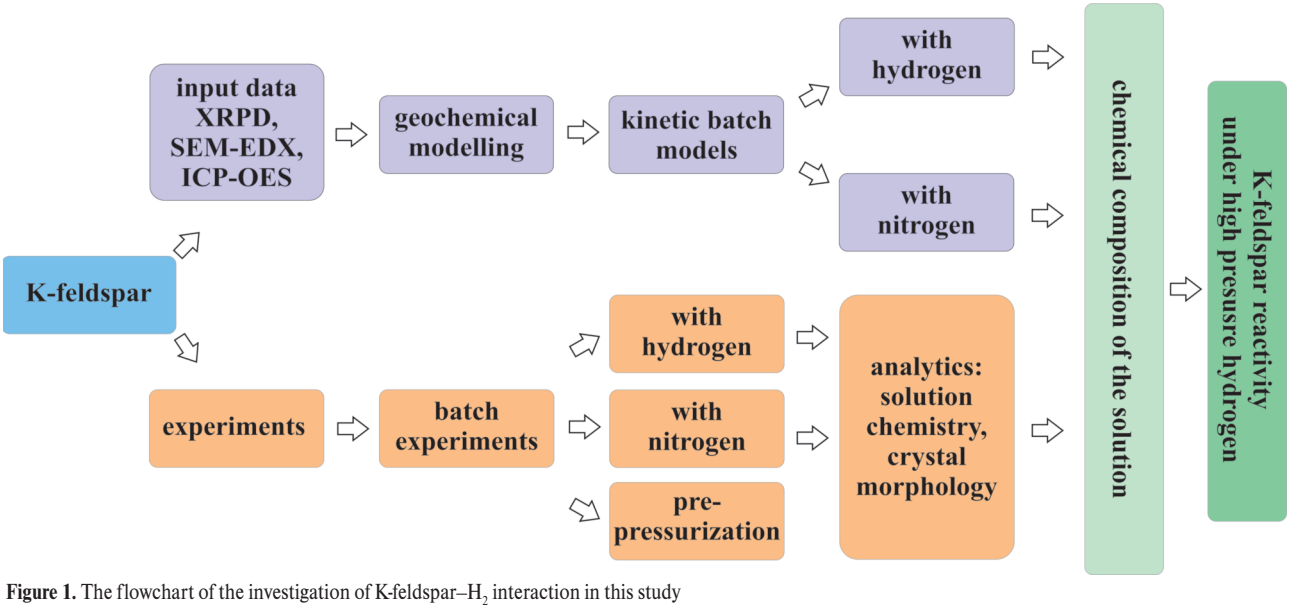

Figure 1. The flowchart of the investigation of K-feldspar–H_2 interaction in this study

1. ábra. *A K-földpát–H_2 kölcsönhatás vizsgálatának elvi ábrája*

heated up to 105 °C and the total system pressure was set to 100 bar. Stirring was continuous with an RPM of 345 min^{-1} during the experiments. At certain reaction times (3, 24, 78 hours), ca. 2 mL of liquid samples were taken via a dip tube for off-line analysis to detect the changes of K^+, Na^+, Si^{4+}, Al^{3+} ion concentrations in the solutions.

Type-2: The same amount of mineral and water was mixed in the reactor vessel for 10 minutes under ambient temperature and pressure conditions to study the fast kinetic processes of mineral dissolution. Since the mixture of Type-1 (mineral and distilled water) spends ca. 10 minutes under room temperature and pressure before pressurization and heating to the reservoir parameters, this experiment was carried out to track the effect of immersion similarly to Stillings et al. (1995). The initial pH and chemical composition of the solution was measured. Thus, the same amount of mineral and water as the Type-1 setup were mixed in the open reactor for 10 minutes. Then the solution was measured and sampled for pH and chemical analysis, respectively. The concentrations obtained from this pre-pressurization experiment served as input data of the geochemical models described below.

For chemical composition analysis of the solution samples, a HORIBA Jobin Yvon® ULTIMA 2C inductively coupled plasma - optical emission spectrometer (ICP-OES) was used at the Supervisory Authority for Regulatory Affairs. The measured concentration values are given as mg/L. The relative error (10%, 20% and 50%) of the concentrations is dependent on the concentration range, with higher errors at concentrations closer to the detection limit.

Geochemical modeling

Modeling concept

Geochemical modeling was carried out using the PHREEQC ver. 3 geochemical software (Parkhurst & Appelo 2013) designed for simulating geochemical reactions in aqueous media. The software integrates thermodynamic equilibrium and kinetic reactions for gas-water-rock interactions. Kinetic dissolution and precipitation equations of mineral phases have been defined similarly to earlier works of the authors (Szabó et al. 2016, 2018). This modeling methodology is primarily based on a USGS report of Palandri & Kharaka (2014).

The thermodynamic data file *phreeqc.dat* was used for the gas-water-mineral reactions at subsurface reservoir temperature and pressure. With input solution composition using the chemical results of the pre-pressurization experiment, kinetic models were run to follow the K-feldspar dissolution in water at 105 °C and 100 bar H_2 similar to experimental conditions (*Figure 1*). The time steps were set for every eight hours from zero to 72 hours in accordance with the sampling times of the experiments.

Model input data

The initial solution compositions and pH used in the models of this study were obtained from the Type-2 experiments. The mixture of K-feldspar and distilled water under room temperature and pressure conditions was sampled for analysis by ICP-OES in order to determine the initial ion concentrations in distilled water before the heating and pressurization experiments. The input solution concentrations of the model are summarized in *Table I*.

Three minerals were defined in the models. The K-feldspar used as experimental substrate was defined as a mixture of sanidine ($KAlSi_3O_8$) and albite ($NaAlSi_3O_8$) in a ratio of 87:13, following the results of SEM-EDX measurement. Furthermore, gibbsite ($Al(OH)_3$) was selected as secondary mineral phase, which may precipitate during the experiments (*Table II*). Specific surface area values of the minerals were manually adjusted based on the data of Gao et al. (2017) and Nebelung & Brendler (2010) for the feldspar, and Bénézeth et al. (2008) for gibbsite.

Table I. Initial temperature, pH and solution composition of the kinetic models that were obtained from pre-pressurization experiments

I. táblázat. *A modellekben definiált oldat bemenő paraméterei (hőmérséklet, pH és a kémiai összetétel), amelyek a rövid, nyomás alá helyezés előtti kísérlet oldatösszetétele alapján lettek meghatározva*

Temperature (°C)	105
pH	6.6
K (mg/L)	1.13
Na (mg/L)	0.06
Al (mg/L)	0.03

Table II. Equilibrium constants, specific surface area (m^2/g) of minerals, and relevant chemical reactions used in the geochemical models of this study

II. táblázat. *A modellezésben használt ásványok listája, azok fajlagos felülete (m^2/g) és egyensúlyi állandóik*

Mineral Phase	Reaction	SSA	Log K
K-feldspar	$KAlSi_3O_8 + 8\ H_2O = K^+ + Al(OH)^{4-} + 3\ H_4SiO_4$	0.09	-20.57
Albite	$NaAlSi_3O_8 + 8\ H_2O = Na^+ + Al(OH)^{4-} + 3\ H_4SiO_4$	0.15	-18.00
Gibbsite	$Al(OH)_3 + 3\ H^+ = Al^{+3} + 3\ H_2O$	1	5.80

Results

Chemical and structural observations on K-feldspar used in experiments

The powdered K-feldspar grains (100-200 m in size) show uniform extinction and birefringence under optical microscope. Similar homogeneity was observed in SEM backscattered images. The mineral composition, obtained by EDX measurements, revealed 87% K-feldspar and 13% albite average composition (*Figure 2*). Since no sign of perthite was observed, and no albite was identified by XRPD, the K-feldspar is interpreted to have formed at elevated temperatures, and at relatively rapid cooling rates. According to the best fit to the XRPD pattern and the chemical data, the K-feldspar is a C2/m high temperature disordered sanidine.

Experimental results

The changes in solution composition during the experiments dominantly indicate continuous dissolution of the K-feldspar grains (*Figure 3*). The solution aliquots collected after 3 h show variations in K concentration from 0.6 to 6.9 mg/L and from 0.7 to 1.4 mg/L in H_2- and N_2-treated runs, respectively. The K^+ content of solutions after 76 hours of H_2 exposure varies from 1.77 to 10.68 mg/L with an average of 6.2 mg/L while it ranges between 1.77 and 8.12 mg/L with an average of 4.8 mg/L in the N_2 experiments. The concentration changes show a slight but consistent increase in the measured ions throughout most of the experiments. The average concentration of K^+ and Na^+ is higher in the H_2-treated samples while the average Si^{4+} and Al^{3+} are higher in N_2 treated sample solutions (*Table III*). Some precipitates were observed by optical microscopy on the surface of the K-feldspar grains in both the H_2 and N_2 experiments. These precipitates can be characterized as rectangular translucent grains ranging from 1 to 5 m in size.

Geochemical modeling results

The model predicts very similar K-feldspar dissolution paths under both H_2 and N_2 pressure. After 72 h, the modeled K^+ concentration in solution reaches 3.2 mg/L with a steep slope (*Figure 3, Table IV*). The concentration of Si rises the steepest among the tested ions. Overall the N_2-run resulted in increased concentrations of all investigated elements (K, Na, Si, Al) compared to the H_2-run. The maximum difference (2.3 mg/L) appears at the end of the runs

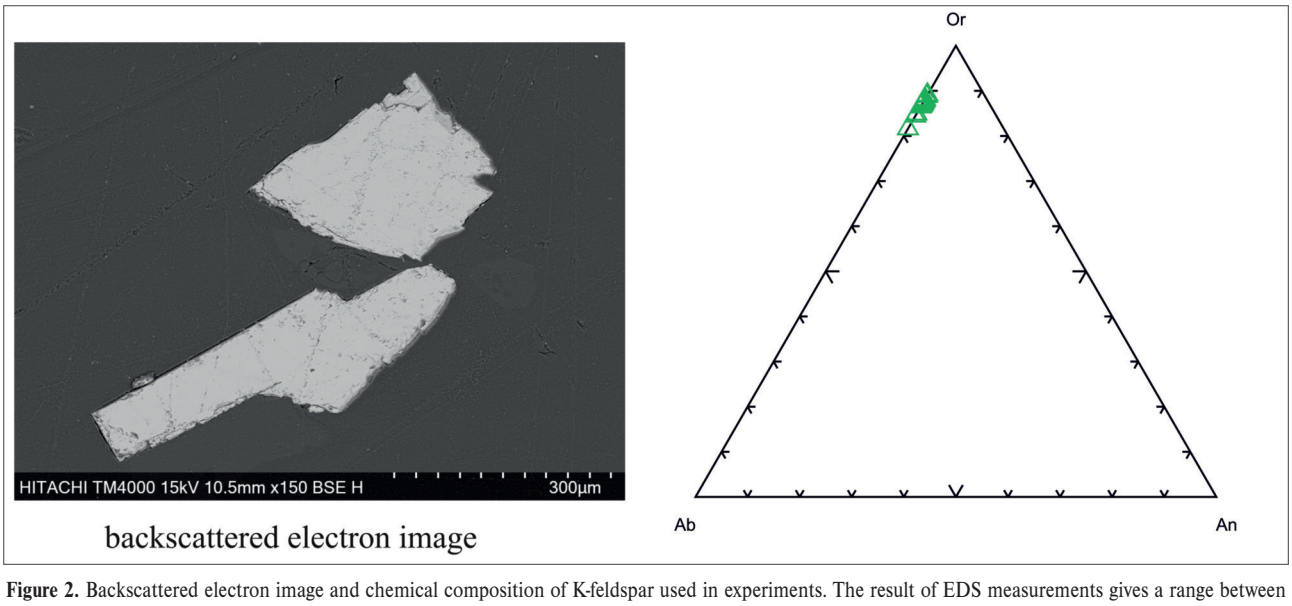

Figure 2. Backscattered electron image and chemical composition of K-feldspar used in experiments. The result of EDS measurements gives a range between Ab_{11}-Ab_{18} content with an average of Ab_{13}

2. ábra. *A kísérletben használt káliföldpát kémiai összetétele energiadiszperzív spektrometriai elemzések alapján. A káliföldpát albitkomponense Ab_{11}-Ab_{18} között változik, átlagosan Ab_{13}*

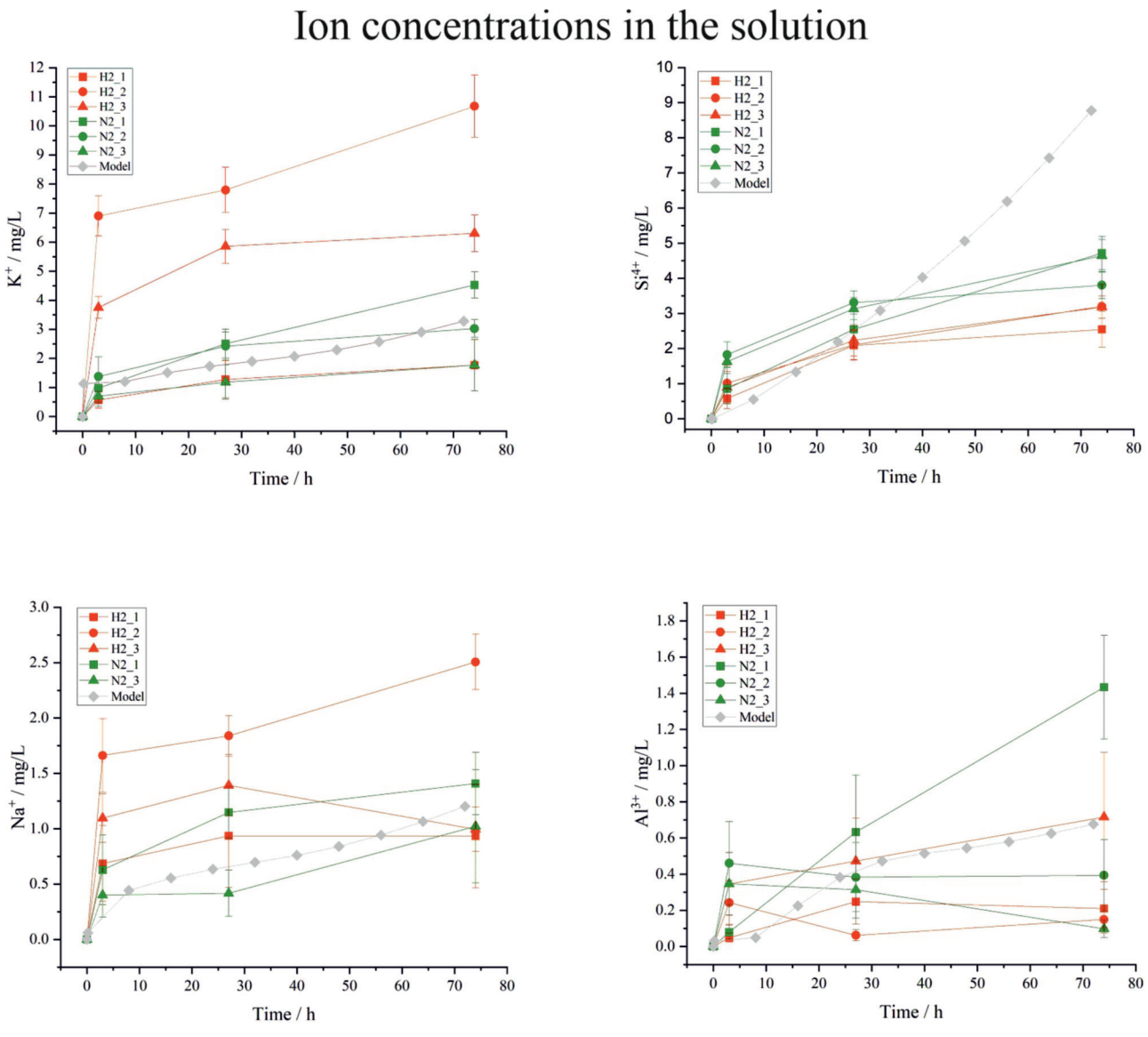

Figure 3. Changes in various ion concentrations (K^+, Na^+, Si^{4+} Al^{3+}) in experiments and in kinetic models

3. ábra. *A különböző ionok koncentrációjának (K^+, Na^+, Si^{4+} Al^{3+}) változása a kísérletekben és a modellekben*

and in the Si concentration (*Table IV*). The model estimates 0.01 wt.% gibbsite precipitation after 72 hours.

Discussion

Discussion of experimental and modeling results

A wealth of data gained from experimental, theoretical, and case studies about the mechanisms of feldspar dissolution (e.g., Wollast & Chou 1992, Stillings & Brantley 1995), processes and kinetics (Wollast 1967), organic and inorganic reaction paths (Carothers & Kharaka 1978), have provided a solid base for understanding rock-water interactions (Yuan et al. 2019). However, there is a lack of experimental study about K-feldspar dissolution that are relevant for the pressure and temperature conditions of subsurface hydrogen storage. Heinrich et al. (1978) carried out mineral-H_2 reactions with silicates, including feldspars, which resulted in the removal of contaminating Fe from the crystal structure. However, since they did not use water in their experiments, their findings are less applicable to underground hydrogen storage studies.

Our results show higher concentrations of K and Na in the fluid samples of the H_2-treated experiments in comparison with the N_2-bearing reference experiments where Si and Al have more elevated concentrations. Kinetic studies have demonstrated that the rate of dissolution of feldspars is promoted by hydrogen ions, and the rate of the dissolution increases as the hydrogen ion concentration increases (e.g., Wollast 1967, Shotyk & Nesbitt 1992).

The ICP-OES results indicate a subtle increase in K and Na dissolution induced by H_2, compared to the outcomes of N_2 experiments (*Figure 3*). Since some precipitates were detected on the samples, a recrystallization process is expected, producing an Al-bearing phase. These results are consistent with those of solution analysis (*Figure 3*) and in-

Table III. ICP-OES results on solution compositions of experiments with H_2 and N_2. The results are grouped by elements and concentrations with error (+/-) given in mg/L. The sampling times are given in hours measured from the beginning of the experiments

III. táblázat. *A kísérletek során vett oldatminták kémiai összetétele az ICP-OES-mérések alapján. Az elemek koncentrációja és a mérési relatív hiba mg/L-ben, míg a kísérlet indításától számított mintázási idő órában van megadva*

Element	Time	H2_1	H2_1 (+/-)	H2_2	H2_2 (+/-)	H2_3	H2_3 (+/-)	N2_1	N2_1 (+/-)	N2_2	N2_2 (+/-)	N2_3	N2_3 (+/-)
K	3	0.57	0.28	6.90	0.69	3.75	0.38	0.97	0.49	1.37	0.69	0.70	0.35
	27	1.28	0.64	7.79	0.78	5.85	0.59	2.51	0.50	2.42	0.48	1.18	0.59
	75	1.77	0.88	10.68	1.10	6.30	0.63	4.53	0.45	3.03	0.30	1.77	0.88
Na	3	0.69	0.34	1.66	0.33	1.10	0.22	0.63	0.31	0.78	0.39	0.40	0.20
	27	0.94	0.47	1.84	0.18	1.39	0.28	1.15	0.23	4.35	0.43	0.42	0.21
	75	0.93	0.47	2.51	0.25	1.00	0.20	1.41	0.28	0.88	0.18	1.02	0.51
Si	3	0.58	0.29	1.02	0.51	0.90	0.45	0.86	0.43	1.82	0.36	1.63	0.16
	27	2.09	0.42	2.10	0.42	2.23	0.45	2.55	0.51	3.31	0.33	3.13	0.31
	75	2.55	0.51	3.20	0.64	3.18	0.32	4.72	0.47	3.80	0.38	4.64	0.46
Al	3	0.05	0.02	0.24	0.12	0.35	0.17	0.08	0.04	0.46	0.23	0.35	0.17
	27	0.25	0.12	0.06	0.03	0.47	0.24	0.63	0.32	0.38	0.19	0.31	0.16
	75	0.21	0.11	0.15	0.07	0.72	0.36	1.43	0.29	0.39	0.20	0.10	0.05

dicate that H_2 has limited effect on K-feldspar dissolution compared to the reference (N_2) experiments at the tested pressures and temperatures.

Moreover, in our experiments non-stochiometric dissolution of the K-feldspar was observed. The dissolution rate is most likely controlled by the development and evolution of a leached layer, built at the surface of the K-feldspar. Reactants and dissolution products can diffuse through this layer, but as the leached layer grows, the diffusion of the leachable species becomes slower, thus, the dissolution rate is slowing down. This phenomenon was first introduced by CORRENS & VON ENGELHARDT (1938) and described later by several studies (WOLLAST 1967, CHOU & WOLLAST 1984, LASAGA 1984). The so-called "preferential leaching-diffusion controlled mechanism" is characterized by a parabolic curved concentration pattern of Al and Si versus time (*Figure 4*). However, ZHU (2005) proposed that the crystallites in the K-feldspar powder may have defects produced by grinding, which may result in non-stoichiometric alterations. Furthermore, our conclusions are limited by the fact that the element concentrations, especially that of Na and Al, are close to the detection limit of the used analytical technique.

Table IV. Variation in ion concentrations (K^+, Na^+, Si^{4+} Al^{3+}) in mg/L of the solutions of the geochemical models with time (h). Results are shown for both hydrogen and nitrogen modeling

IV. táblázat. *Elemösszetételek (mg/L) időbeli változásai a geokémiai modellekben - mind hidrogénnel és nitrogénnel*

	time	pH	K	Na	Si	Al
Hydrogen	8	7.35	1.21	0.44	0.55	0.05
	16	7.47	1.51	0.55	1.33	0.23
	24	7.51	1.73	0.63	2.18	0.38
	32	7.55	1.90	0.70	3.08	0.47
	40	7.61	2.07	0.76	4.03	0.52
	48	7.68	2.29	0.84	5.06	0.54
	56	7.76	2.57	0.94	6.19	0.58
	64	7.83	2.91	1.06	7.43	0.62
	72	7.89	3.28	1.20	8.78	0.68
Nitrogen	8	7.35	1.31	0.48	0.77	0.10
	16	7.47	1.64	0.60	1.76	0.32
	24	7.51	1.87	0.69	2.81	0.48
	32	7.55	2.08	0.76	3.92	0.57
	40	7.61	2.33	0.85	5.12	0.63
	48	7.68	2.64	0.97	6.42	0.68
	56	7.76	3.03	1.11	7.85	0.75
	64	7.83	3.46	1.27	9.40	0.83
	72	7.89	3.94	1.44	11.08	0.91

Based on the experiments the following steps are expected to take place according to OELKERS et al. (2008) and OELKERS & SCHOTT (1995):

1) Relatively rapid exchange of hydrogen and alkali ions near the mineral surface causing elevated K and Na concentrations in H_2-treated experiments compared to the reference material.

2) Exchange reaction between three hydrogen atoms from the solution with one aluminum atom of the mineral structure, resulting in the breaking of Al-O bonds, coupled with the formation of a rate-controlling Si-rich precursor complex.

3) Hydrolysis of Si-O bonds. The removal of Si still requires the breaking of Si-O bond and thus the overall alkali feldspar dissolution rate is controlled by the decomposition of a silica-rich surface precursor in geochemical systems at far from equilibrium conditions.

Comparison of modeling and laboratory observations

The geochemical modeling shows less pronounced variation in ion concentrations (K, Na, Al, Si) between the H_2 and reference runs (*Table IV*). The modeling predictions for solution concentration curves are close to experimental averages, except in the case of dissolved Si (*Figure 3*). The models do not consider any retention on the surface of the minerals. Although gibbsite was allowed to precipitate as secondary mineral phase, the layered nature of dissolution mechanism was not considered in the modeling. Therefore, the Si concentration does not reach a plateau, like in the experiments, rather it tends to increase linearly. These discrepancies could originate from the thermodynamic database used in this modeling study. It is known that thermodynamic properties of minerals derived from calorimetric and phase equilibrium experiments rarely predict experimental solubility results accurately (SVERJENSKY et al.

1991). Zhu & Lu (2009) concluded that deriving proper rate laws from experiments is still difficult for feldspar-water systems especially to describe the precipitation rates of secondary phases. However, our results seem to be applicable for further more intricate hydrogen storage simulations where bulk rock composition and formation water are considered.

Relevance of results in underground hydrogen storage and the way forward to more complex systems

Feldspar alteration can result in various diagenetic mineral assemblages under different physicochemical conditions (Yuan et al. 2019). If a new reactive gas phase (H_2, CO_2) intrudes into the pore space it can cause further feldspar-related chemical reactions (Henkel et al. 2014, Tutolo et al. 2015).

The low-temperature dissolution of natural K-feldspars in aqueous media is extremely slow (Lasaga 1984, Liu & Zhai 2021). However, the chemical reaction time is sharply shortened (to a few hours or tens of hours) for K-feldspar under extreme hydrothermal conditions (Liu et al. 2015). The effect of H_2 on reservoir rocks containing K-feldspar has already been studied experimentally and these authors concluded that no or abiotic interactions take place with H_2 (Yekta et al. 2018, Hassanpouryouzband et al. 2022, Flesch et al. 2018). However, these experimental studies are based on whole rock samples with complex mineralogical compositions, hence it is difficult to directly apply their conclusions.

K-feldspar promoted illitization in interbedded mudstones by supplying K^+ is also observed in diagenetic environments (Yuan et al. 2019). Considering increased K^+ and Na^+ dissolution compared to N_2-bearing experiments, it can be assumed that H_2 addition into the solution will decrease the pH and therefore the dissolution of feldspar will be more intense. Accordingly, in the abundance of H^+ ions, the mineral surface reactions can be enhanced. In a polymineralic rock under diagenetic conditions, the K^+ released from feldspar can enter the illite structure thus causing pore clogging. Moreover, the experiments demonstrated that the Al released from the K-feldspar immediately forms a solid phase and does not prefer the solution indicating that Al, dissolved from K-feldspar, is a source of aluminosilicate secondary phases, which can cause further pore clogging. Consequently, the newly forming aluminosilicates can reduce the porosity and permeability of the reservoir. The possible decline of these latter two parameters may adversely affect both the void space and the injectivity of the subsurface storage unit.

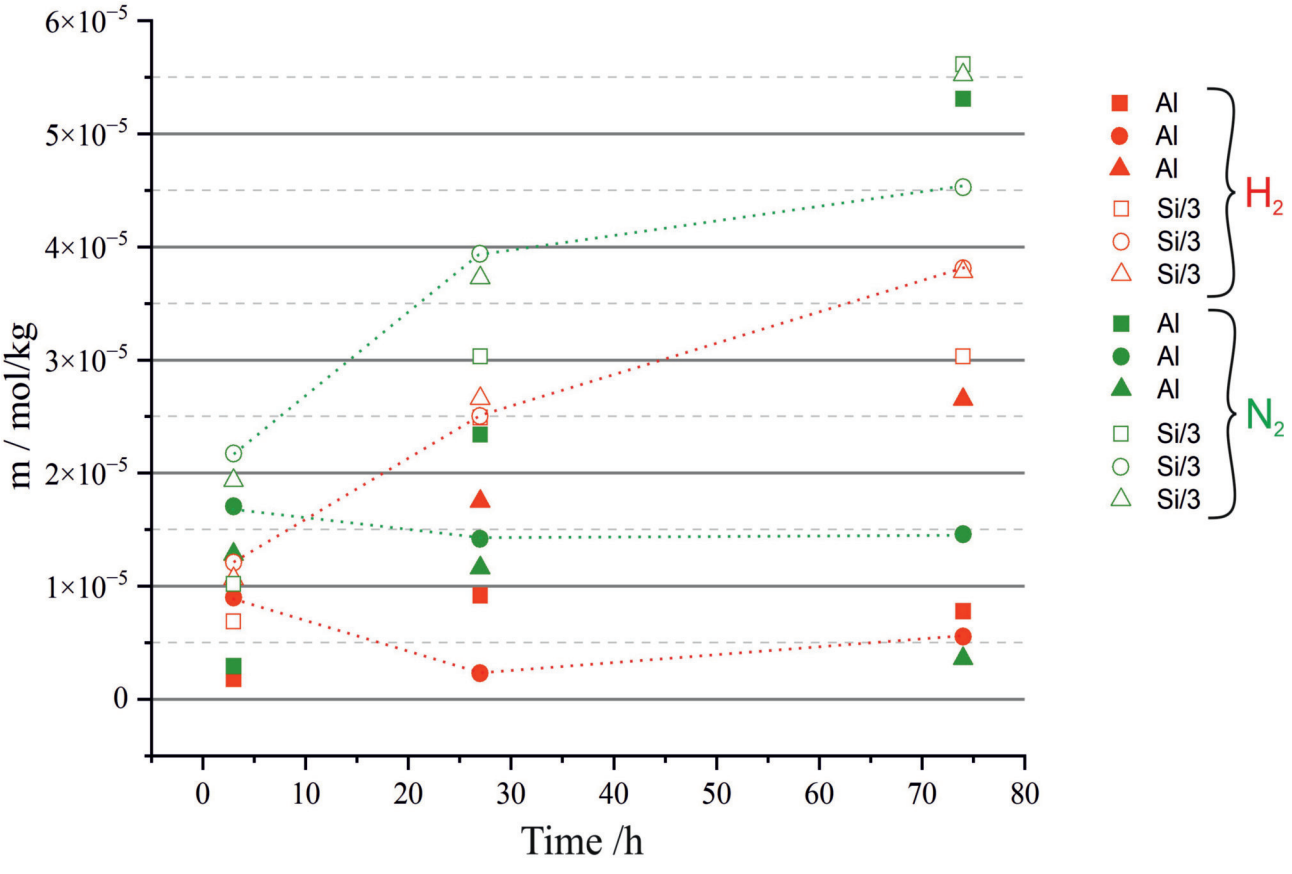

Figure 4. Change in element concentrations (in mol/kg) during experiments. The filled symbols denote Al concentrations, while open symbols show Si/3 concentrations of experiments with H_2 (red) and N_2 (green)

4. ábra. *Oldatmintáink alumínium- és szilícium/3-tartalmának (mol/kg) változása a kísérletekben. Teli szimbólumok jelölik az Al-koncentrációt, míg az üresek a Si/3-koncentrációt az egyes kísérletekben*

Conclusion

This combined experimental-modeling study focused on the geochemical impact of hydrogen on K-feldspar under subsurface hydrogen storage conditions (105 °C and 100 bar). Our experimental data show a limited effect of hydrogen on K-feldspar compared to reference experiments with nitrogen. The kinetic PHREEQC model predicts the dissolution of K-feldspar to a similar extent as suggested by the experimental observations. Findings of this study show that the K-feldspar-hydrogen interaction results in an increased release of K and Na and the formation of an Al-bearing mineral phase. In the context of a complex subsurface reservoir environment, the results may suggest that hydrogen injection can slightly increase K-feldspar dissolution, hence supplying ions for secondary mineral precipitation.

It is worth noting that our experiments are oversimplified, while the bulk rock experiments are too short-lived to yield far-reaching conclusions, given the intricate nature of the system. As a next step, the experiments should be made more complex via introducing a new mineral phase or using solution compositions that are more similar to reservoir fluids.

Acknowledgements

This article is a tribute to Csaba SZABÓ's oeuvre. He taught generations to understand the geochemical processes with a passion which has inspired numerous students to start scientific career, including many of the authors (D. BREITNER, Gy. FALUS, O. GELENCSÉR, Á. KŐVÁGÓ, Zs. SZABÓ-KRAUSZ). He is not only a great educator, but he has also opened new avenues for scientific exploration which is demonstrated by his pivotal role in paving the way of rock-porewater and-gas interaction studies in Hungary.

We thank the two anonymous reviewers for their helpful comments and suggestions, and Orsolya SZTANÓ for her valuable editorial work.

Project no. 971238 has been implemented with the support provided by the Ministry of Culture and Innovation of Hungary from the National Research, Development and Innovation Fund, financed under the KDP-2020 funding scheme. This work was supported by O&GD Central Ltd., Budapest, Hungary. The Project was partially supported by the Hungarian National Research, Development, and Innovation Office – NKFIH under FK 143197 grant.

References – Irodalom

AL-YASERI, A., AL-MUKAINAH, H., YEKEEN, N. & AL-QASIM, A. S. 2023: Experimental investigation of hydrogen-carbonate reactions via computerized tomography: Implications for underground hydrogen storage. – *International Journal of Hydrogen Energy* **48/9**, 3583–3592. https://doi.org/10.1016/j.ijhydene.2022.10.148

BEHRENS, H. 2021: Hydrogen defects in feldspars: kinetics of D/H isotope exchange and diffusion of hydrogen species in alkali feldspars. – *Physics and Chemistry of Minerals* **48/8**, 1–23. https://doi.org/10.1007/s00269-021-01150-w

BÉNÉZETH, P., PALMER, D. A. & WESOLOWSKI, D. J. 2008: Dissolution/precipitation kinetics of boehmite and gibbsite: Application of a pH-relaxation technique to study near-equilibrium rates. – *Geochimica et Cosmochimica Acta* **72/10**, 2429–2453. https://doi.org/10.1016/j.gca.2008.02.019

BENISEK, A., KROLL, H. & CEMIC, L. 2004: New developments in two-feldspar thermometry. – *American Mineralogist* **89**, 1496–1504. https://doi.org/10.2138/am-2004-1018

BERNER, R. A. 1995: Chemical Weathering and Its Effect on Atmospheric CO_2 and Climate. – In: WHITE, A. F. & BRANTLEY, S. L. (Eds.): *Chemical Weathering Rates of Silicate Minerals* Vol. 31, 565–584, Washington D.C., Mineralogical Society of America. https://doi.org/10.1515/9781501509650-015

CAROTHERS, W. W. & KHARAKA, Y. K. 1978: Aliphatic Acid Anions in Oil-Field Waters – Implications for Origin of Natural Gas. – *AAPG Bulletin* **62/12**, 2441–2453. https://doi.org/10.1306/C1EA5521-16C9-11D7-8645000102C1865D

CHARDON, E. S., LIVENS, F. R. & VAUGHAN, D. J. 2006: Reactions of feldspar surfaces with aqueous solutions. – *Earth-Science Reviews* **78/1–2**, 1–26. https://doi.org/10.1016/j.earscirev.2006.03.002

CHOU, L. & WOLLAST, R. 1984: Study of the weathering of albite at room temperature and pressure with a fluidized bed reactor. – *Geochimica et Cosmochimica Acta* **48/11**, 2205–2217. https://doi.org/10.1016/0016-7037(84)90217-5

CORRENS, C. W. & VON ENGELHARDT, W. 1938: Neue Untersuchungen fiber die Verwitterung. – *Naturwissenschaften* **230**, 137–138. https://doi.org/10.1007/BF01772798

FLESCH, S., PUDLO, D., ALBRECHT, D., JACOB, A. & ENZMANN, F. 2018: Hydrogen underground storage – Petrographic and petrophysical variations in reservoir sandstones from laboratory experiments under simulated reservoir conditions. – *International Journal of Hydrogen Energy* **43/45**, 20822–20835. https://doi.org/10.1016/j.ijhydene.2018.09.112

FUERTES, V., REINOSA, J. J., FERNÁNDEZ, J. F. & ENRÍQUEZ, E. 2022: Engineered feldspar-based ceramics: A review of their potential in ceramic industry. – *Journal of the European Ceramic Society* **42/2**, 307–326. https://doi.org/10.1016/j.jeurceramsoc.2021.10.017

GAO, X., BI, M., SHI, K., CHAI, Z. & WU, W. 2017: Sorption characteristic of uranium(VI) ion onto K-feldspar. – *Applied Radiation and Isotopes* **128**, 311–317. https://doi.org/10.1016/j.apradiso.2017.07.041

GELENCSÉR, O., ÁRVAI, C., MIKA, L. T., BREITNER, D., LECLAIR, D., SZABÓ, C., FALUS, G. & SZABÓ-KRAUSZ, Z. 2023: Effect of hydrogen on calcite reactivity in sandstone reservoirs: Experimental results compared to geochemical modeling predictions. – *Journal of Energy Storage* **61**, 1–6. https://doi.org/10.1016/j.est.2023.106737

HASSANPOURYOUZBAND, A., ADIE, K., COWEN, T., THAYSEN, E. M., HEINEMANN, N., BUTLER, I. B., WILKINSON, M. & EDLMANN, K. 2022: Geological Hydrogen Storage: Geochemical Reactivity of Hydrogen with Sandstone Reservoirs. – *ACS Energy Letters* **7**, 2203–2210. https://doi.org/10.1021/acsenergylett.2c01024

HEINEMANN, N., ALCALDE, J., MIOCIC, J. M., HANGX, S. J. T., KALLMEYER, J., OSTERTAG-HENNING, C., HASSANPOURYOUZBAND, A., THAYSEN, E. M., STROBEL, G. J., SCHMIDT-HATTENBERGER, C., EDLMANN, K., WILKINSON, M., BENTHAM, M., STUART HASZELDINE, R.,

Carbonell, R. & Rudloff, A. 2021: Enabling large-scale hydrogen storage in porous media-the scientific challenges. – *Energy and Environmental Science* **14/2**, 853–864. https://doi.org/10.1039/D0EE03536J

Heinrich, E. W., Salotti, C. A. & Giardini, A. A. 1978: Hydrogen-mineral reactions and their application to the removal of iron from spodumene. – *Energy* **3/3**, 273–279.

Henkel, S., Pudlo, D., Werner, L., Enzmann, F., Reitenbach, V., Albrecht, D., Würdemann, H., Heister, K., Ganzer, L. & Gaupp, R. 2014: Mineral reactions in the geological underground induced by H_2 and CO_2 injections. – *Energy Procedia* **63**, 8026–8035.

Lasaga, A. C. 1984: Chemical Kinetics of Water-Rock Interactions. – *Journal of Geophysical Research* **89/4**, 4009–4025. https://doi.org/10.1029/JB089iB06p04009

Liu, S. K., Han, C., Liu, J. M. & Li, H. 2015: Hydrothermal decomposition of potassium feldspar under alkaline condition. – *RSC Advances* **5**, 93301–93309. https://doi.org/10.1039/C5RA17212H

Liu, S., Qi, X., Han, C., Liu, J., Sheng, X., Li, H., Luo, A. & Li, J. 2017: Novel nano-submicron mineral-based soil conditioner for sustainable agricultural development. – *Journal of Cleaner Production* **149**, 896–903. https://doi.org/10.1016/j.jclepro.2017.02.155

Liu, S. & Zhai, Y. 2021: Degree of Al-Si order in K-feldspar and its effect on K-feldspar's dissolution. – *Periodico di Mineralogia* **90/3**, 359–369.

Manning, D. A. C., Baptista, J., Sanchez Limon, M. & Brandt, K. 2017: Testing the ability of plants to access potassium from framework silicate minerals. – *Science of the Total Environment* **574**, 476–481. https://doi.org/10.1016/j.scitotenv.2016.09.086

Nebelung, C. & Brendler, V. 2010: U(VI) sorption on granite: Prediction and experiments. – *Radiochimica Acta* **98/9–11**, 621–625. https://doi.org/10.1524/ract.2010.1762

Oelkers, E. H. & Schott, J. 1995: Experimental study of anorthite dissolution and the relative mechanism of feldspar hydrolysis. – *Geochimica et Cosmochimica Acta* **59/24**, 5039–5053. https://doi.org/10.1016/0016-7037(95)00326-6

Oelkers, E. H., Schott, J., Gauthier, J. M. & Herrero-Roncal, T. 2008: An experimental study of the dissolution mechanism and rates of muscovite. – *Geochimica et Cosmochimica Acta* **72/20**, 4948–4961. https://doi.org/10.1016/j.gca.2008.01.040

Palandri, J. L. & Kharaka, Y. K. 2004: A compilation of rate parameters of water-mineral interaction kinetics for application to geochemical modeling. – *USGS Open File Report* **2004–1068**, 71.

Parkhurst, D. L. & Appelo, C. A. J. 2013: Description of input and examples for PHREEQC version 3: a computer program for speciation, batch-reaction, one-dimensional transport, and inverse geochemical calculations. – *U.S. Geological Survey Techniques and Methods*, book 6, chap. A43, 497 p.

Putnis, A. 1992: The crystal structure of minerals – I. – In: Putnis, A. (Ed.): *An Introduction to Mineral Sciences*, 121–140, Cambridge: Cambridge University Press.

Ribbe, P. H. 1994: The Crystal Structures of the Aluminum-Silicate Feldspars. – In: Parsons, I. (Ed.): *Feldspars and their Reactions*, NATO ASI S., 1–49, Springer. https://doi.org/10.1007/978-94-011-1106-5_1

Shotyk, W. & Nesbitt, H. W. 1992: Incongruent and congruent dissolution of plagioclase feldspar: effect of feldspar composition and ligand complexation. – *Geoderma* **55/1–2**, 55–78. https://doi.org/10.1016/0016-7061(92)90005-R

Stillings, L. L. & Brantley, S. L. 1995: Feldspar dissolution at 25 °C and pH 3: Reaction stoichiometry and the effect of cations. – *Geochimica et Cosmochimica Acta* **59/8**, 1483–1496. https://doi.org/10.1016/0016-7037(95)00057-7

Stillings, L. L., Brantley, S. L. & Machesky, M. L. 1995: Proton adsorption at an adularia feldspar surface. – *Geochimica et Cosmochimica Acta* **59/8**, 1473–1482. https://doi.org/10.1016/0016-7037(95)00056-6

Sverjensky, D. A., Hemley, J. J. & D'angelo, W. M. 1991: Thermodynamic assessment of hydrothermal alkali feldspar-mica-aluminosilicate equilibria. – *Geochimica et Cosmochimica Acta* **55/4**, 989–1004. https://doi.org/10.1016/0016-7037(91)90157-Z

Szabó, Z., Hellevang, H., Király, C., Sendula, E., Kónya, P., Falus, G., Török, S. & Szabó, C. 2016: Experimental-modelling geochemical study of potential CCS caprocks in brine and CO_2-saturated brine. – *International Journal of Greenhouse Gas Control* **44**, 262–275. https://doi.org/10.1016/j.ijggc.2015.11.027

Szabó, Z., Gál, N. E., Kun, É., Szőcs, T. & Falus, G. 2018: Accessing effects and signals of leakage from a CO_2 reservoir to a shallow freshwater aquifer by reactive transport modelling. – *Environmental Earth Sciences* **77/12**. https://doi.org/10.1007/s12665-018-7637-6

Tutolo, B. M., Luhmann, A. J., Kong, X. Z., Saar, M. O. & Seyfried, W. E. 2015: CO_2 sequestration in feldspar-rich sandstone: Coupled evolution of fluid chemistry, mineral reaction rates, and hydrogeochemical properties. – *Geochimica et Cosmochimica Acta* **160**, 132–154. https://doi.org/10.1016/j.gca.2015.04.002

Welch, S. A. & Ullman, W. J. 1996: Feldspar dissolution in acidic and organic solutions: Compositional and pH dependence of dissolution rate. – *Geochimica et Cosmochimica Acta* **60/16**, 2939–2948. https://doi.org/10.1016/0016-7037(96)00134-2

Wollast, R. 1967: Kinetics of the alteration of K-feldspar in buffered solutions at low temperature. – *Geochimica et Cosmochimica Acta* **31/4**, 635–648. https://doi.org/10.1016/0016-7037(67)90040-3

Wollast, R. & Chou, L. 1992: Surface reactions during the early stages of weathering of albite. – *Geochimica et Cosmochimica Acta* **56/8**, 3113–3121. https://doi.org/10.1016/0016-7037(92)90292-Q

Yekta, A. E., Pichavant, M. & Audigane, P. 2018: Evaluation of geochemical reactivity of hydrogen in sandstone: Application to geological storage. – *Applied Geochemistry* **95/May**, 182–194. https://doi.org/10.1016/j.apgeochem.2018.05.021

Yuan, G., Cao, Y., Schulz, H. M., Hao, F., Gluyas, J., Liu, K., Yang, T., Wang, Y., Xi, K. & Li, F. 2019: A review of feldspar alteration and its geological significance in sedimentary basins: From shallow aquifers to deep hydrocarbon reservoirs. – *Earth-Science Reviews* **191/February**, 114–140. https://doi.org/10.1016/j.earscirev.2019.02.004

Zhu, C. 2005: In situ feldspar dissolution rates in an aquifer. – *Geochimica et Cosmochimica Acta* **69/6**, 1435–1453. https://doi.org/10.1016/j.gca.2004.09.005

Zhu, C. & Lu, P. 2009: Alkali feldspar dissolution and secondary mineral precipitation in batch systems: 3. Saturation states of product minerals and reaction paths. – *Geochimica et Cosmochimica Acta* **73/11**, 3171–3200. https://doi.org/10.1016/j.gca.2009.03.015

Zivar, D., Kumar, S. & Foroozesh, J. 2021: Underground hydrogen storage: A comprehensive review. – *International Journal of Hydrogen Energy* **46/45**, 23436–23462. https://doi.org/10.1016/j.ijhydene.2020.08.138

Manuscript received: 05/03/2024

Appendix

Appendix S1. Detailed description of the mineral amount conversion from mol/kgW (PHREEQC model output) to wt.%. The calculation derived from SZABÓ et al. (2018) as follows:

$$c_{mineral}[wt.\%] = \frac{c_{mineral}\left[\frac{mol}{kgW}\right] * M_{mineral}\left[\frac{g}{mol}\right] * vol\%_{water}}{10 * \rho_{rock}\left[\frac{g}{cm^3}\right] * vol\%_{rock}}$$

where $c_{mineral}$ is the concentration of the mineral, $M_{mineral}$ is the molar mass of the mineral in g/mol, the density (ρ) of the rock is in g/cm^3, the rock-water ratio is in vol%.

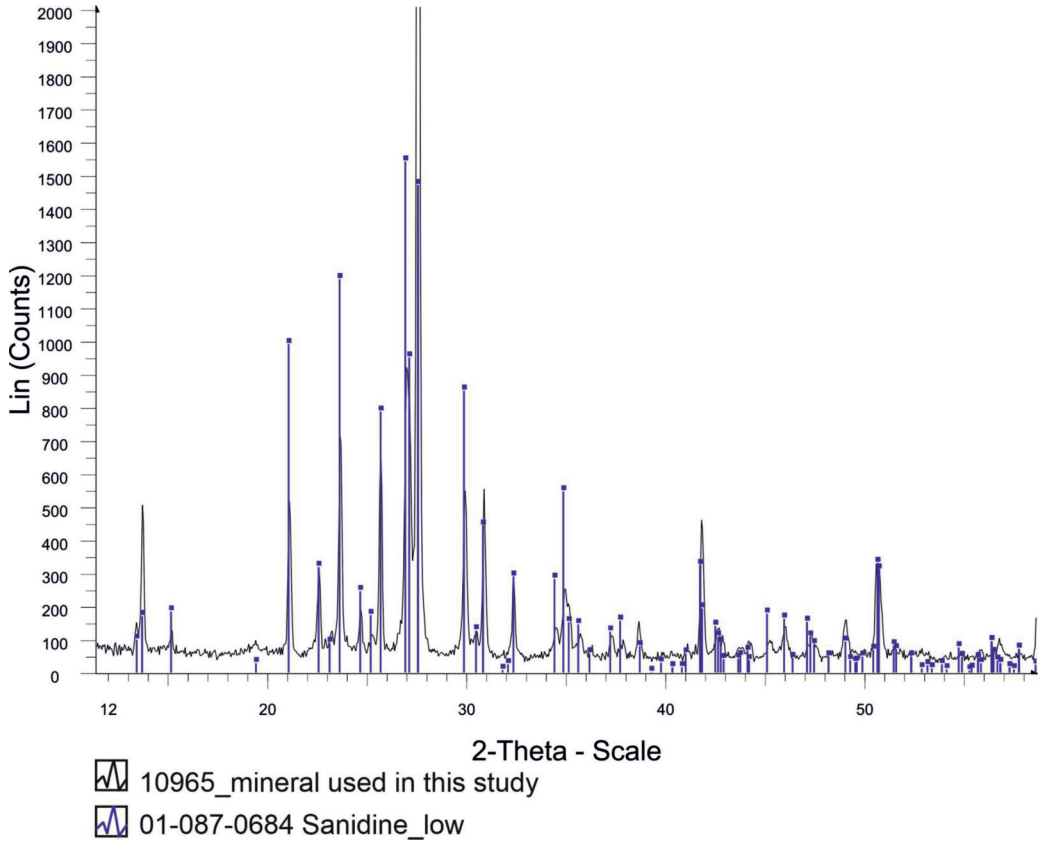

Figure S1. Diffractogram (black) of the mineral used in this study collected by X-ray powder diffraction (XRPD) method and the standard sanidine peak positions (blue) is also shown for comparison

S1. ábra. *Diffraktogram (fekete) a kísérletben használt ásványról röntgen pordiffrakciós (XRPD) technikával, továbbá szanidin standard csúcspozíciói (kék) vannak feltüntetve összehasonlításképpen*

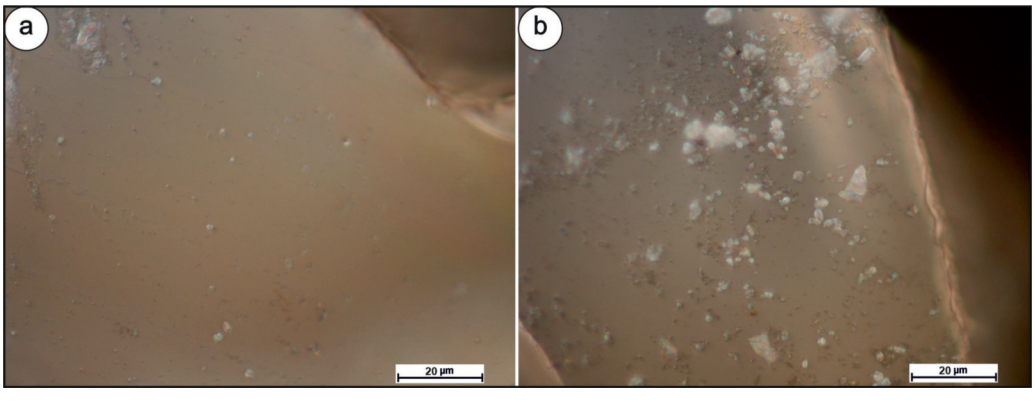

Figure S2. Photomicrographs of K-feldspar grain surfaces. a. K-feldspar grain surface before the experiment. b. K-feldspar grain surface after N2 experiment. Rectangular translucent precipitates showed up on the K-feldspar surface with a size between 1 and 5 µm

S2. ábra. *Optikai mikroszkópos felvétel földpátszemcsékről. a) földpátszemcse felszíne kísérlet előtt. b) földpátszemcse felszíne kísérlet után. A földpát felszínén áttetsző szögletes kristályok láthatók, amelyek mérete 1 és 5 µm között változik*